Synthesis and Characterization of TiO₂ Semiconductor Doped by AgNO₃ and Their Application as Photoanode in Dye-sensitized Solar Cells

Marjoni Imamora Ali Umar[*1)], Nanda Faizil[1)], Akrajas Ali Umar[2)], Siti Khatijah Md Saad[2)]

[*1)] Department of Physics Education, Faculty of Tarbiyah and Teacher Training (FTIK), Institut Agama Islam Negeri (IAIN) Batusangkar, 27213, West Sumatera, Indonesia
[2)] Institute of Microengineering and Nanoelectronics (IMEN), Universiti Kebangsaan Malaysia (UKM), Bangi, Selangor Darul Ehsan, Malaysia

Corresponding Author Email: marjoni.imamora@iainbatusangkar.ac.id; Tel.: +62752-71150; fax: +62752-71879

Abstract
The use of Titanium dioxide (TiO₂) semiconductors in Dye-Sensitized Solar Cells (DSSC) devices have been extensively studied and synthesized with various techniques to obtain optimal performance. The TiO₂ semiconductors with optimal performance are influenced by the growth method, the time of growth, the shape of the microstructure, and the optical properties. In this study, it was reported about the effect of silver nanoparticles (AgNO₃) doping onto TiO₂ semiconductors on their microstructure, reflectance, and efficiency of the DSSC device. The synthesis of TiO₂ was carried out using liquid phase deposition (LPD) and immersed into an AgNO₃ solution with a variation of time namely 0.5 h, 1 h, 2 h, 4 h, and 6 h. The entire TiO2 + AgNO₃ sample, then used as a photoanode on DSSC with plastisol as a counter electrode. Characterization of microstructure, reflectance, and DSSC performance was carried out by using field emission scanning electron microscopy (FESEM), Uv-Vis Spectrophotometer, and Gamry Instrument, respectively. The FESEM results show that AgNO₃ has successfully grown on the ITO substrate in a spherical shape with an average particle diameter ranging from 1.52-2.29 μm. From observations using the Uv-Vis Spectrophotometer, obtained the energy band gap values ranged from 0.22 to 2.27 eV. The best results of DSSC device efficiency, with TiO₂+AgNO₃/Dye/Plastisol structure, have resulted in the Voc of 0.694 V, current density (Jsc) of 0,943 mA/cm² and *fill factor* (FF) of 43,50% which is obtained at sample 1.

INTRODUCTION

The energy crisis in the current technological era is one of the challenges that is being faced and needs efforts to develop alternative energy. One of the alternative energy that has a potential source but has not been maximally utilized is energy comes from sunlight. To harness energy from sunlight is through a device known as a solar cell. Solar cells work by directly converting solar radiation into electricity. The widely used solar cells are silicon-based which are the result of the rapid development of electronic semiconductor technology. Solar cells dominated by silicon have a disadvantage especially the cost of synthesis is more expensive than fossil energy sources. Besides, during the synthesis

process, there is the use of hazardous chemicals (Zamrani et al., 2013). With these weaknesses, the researchers are trying to develop solar cells to replace silicon-based solar cells, such as DSSC (M. I. A. Umar et al., 2017). DSSC has the advantage of not requiring high purity semiconductor materials so that the production costs are relatively low (Septina, 2007), and the manufacturing process does not use chemicals that are dangerous and environmentally friendly.

The most widely used semiconductor in DSSC devices is TiO_2 and Zinc Oxide (ZnO) because they have a wide bandgap. ZnO is a semiconductor that has a fairly wide bandgap of 3.37 eV (Kao et al., 2007), while on TiO_2, it has a bandgap energy of 3.2 eV (Asahi et al., 2001)). At present, the use of TiO_2 as a semiconductor has been widely developed because it can provide better efficiency, inexpensive, photo corrosion resistance, and has good optical characteristics (Grätzel, 2003). TiO_2 semiconductors that are used today have been developed by modification through the addition of metal or doping in small amounts that can change the material properties (M. I. A. Umar, 2019). One of the metals that are widely added to the synthesis of TiO_2 nanoparticles is to use silver nitrate ($AgNO_3$). The $AgNO_3$ doping also aims to reduce pore size, and broaden the surface of the catalyst so that it can optimize the activity of TiO_2. Besides doping $AgNO_3$ nanoparticles on TiO_2, causing changes in the characterization of TiO_2 particles such as size, and particle morphology (Das et al, 2009). The size and shape of TiO_2 nanoparticles are very important in determining the optical, electrical, magnetic, and semiconductor catalysts of TiO_2. Factors that can affect particle size in synthesis are solution temperature, solution concentration (Šileikaitė et al., 2006).

Generally, TiO_2 has three phases namely rutile, anatase, and brookite (Mo et al., 1995). Anatase TiO_2 crystals have more active than rutile. The anatase phase is considered the most favorable phase for photocatalyst and solar energy conversion (Ekasari et al., 2013). The use of TiO_2 with the anatase phase in its application to DSSC has the potential to achieve higher efficiency. Based on the synthesis process carried out for 1 hour by precipitating a growth solution for 24 hours, it can produce a semiconductor TiO_2 with an anatase phase that has a high dielectric constant (e = 80) and the size of the nanoparticles between 14-16 nm (Ekasari & Yudoyono, 2013). Treatment with the addition of $AgNO_3$ doping onto the TiO_2 film with variations in growth time may promise to change the resulting semiconductor characterization. This is proven by FESEM results showed that the presence of silver nanoparticles on an ITO substrate in a spherical shape with particle diameters ranging from 1.52-2.29 μm. Uv-Vis spectrophotometer also provides data on the value of the energy bandgap or bandgap ranging from 0.22 to 2.27 eV. Besides that, the achievements of DSSC devices were also analyzed using $AgNO_3$-supported TiO_2 as photo-anode which are discussed in detail in the results and discussion section.

METHOD
Material and characterization
The main chemicals used include silver nitrate ($AgNO_3$) as doping, boric acid (H_3BO_3), and Potassium Titanyl Phosphate (KTP / $KTiOPO_4$) as precursors. The use of plastisol as the main material in the manufacture of counter electrodes (CE). All of this research material was purchased from Sigma-Aldrich and used directly without prior purification. The research equipment used includes Spin-coater, Uv-Vis Spectrophotometer, and Field Emission Scanning Electron Microscope (FESEM) and Gamry Instrument.

Synthesis Procedure of TiO₂ + AgNO₃
To conduct the synthesis process, we used the substrate, and bottles used have been cleaned first. In the TiO2 synthesis process, the addition of silver nitrate ($AgNO_3$) in the form of small white beads is used. The addition of silver particles is carried out utilizing

$AgNO_3$ reduction with H_3BO_3 and KTP. $AgNO_3$ nanoparticle growth was carried out by varying the effect of time by making a solution with the following steps, as much as 0.0136 grams of AgNO3 mixed with 4 mL of Deionized Water (DI), as much as 0.124 gr H_3BO_3 yang mixed with 20 mL DI, 0.6 gr KTP yang mixed with 20 mL DI. These three solutions were mixed and put the substrate which had grown by TiO_2 into these solutions with a variations growth time of 0.5 h, 1 h, 2 h, 4 h, and 6 h. The TiO2 nanoparticles were first grown using the Liquid Phase Deposition (LPD) method. This method grows TiO_2 nanoparticles in a wise bath with a temperature of 80^0C. After reaching the specified time, the substrate is dried and Annealing for 4 hours at 400^0C. The complete procedure on the method of growing TiO_2 has been well described by previous researchers (A. A. Umar et al., 2018).

Counter electrodes (CE) were synthesized using the spin coating method. This method grows platinum (Pt) on the substrate by placing the substrate on the Spin-coater and then dripping with 1 mL plastisol. Then spin with a speed of 1500 rpm and put into Petri dish which has been wrapped in aluminum foil and heated on a hot plate for 15 minutes. This process is carried out 3 times to get a thick layer of platinum. After that, annealing in the furnace for 1 hour at 400^0C.

RESULTS AND DISCUSSION

Fig. 1 shows the microstructure shape of resultant TiO_2 obtained from the FESEM image at a magnification of 5000 times with variations in the time of preparation of growth for each sample that is 0.5, 1, 2, 4 and 6 hours. In Fig. 1, the difference in FESEM results obtained from the TiO_2 film without doping (a) and (b-f) TiO_2 with $AgNO_3$ doping with variations in growth time.
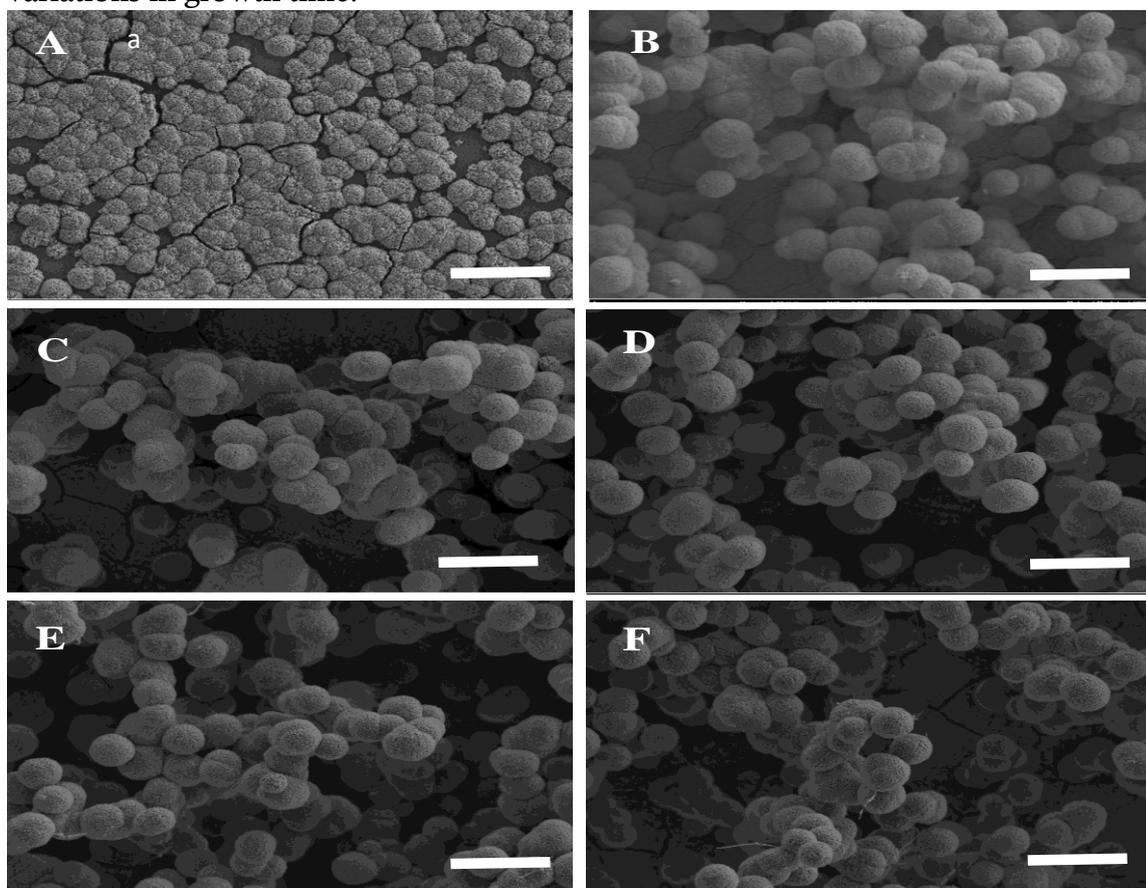
Figure 1. FESEM of (a) TiO_2, (b-f) by doping $AgNO_3$ with variations in growth time from 0.5 h, 1 h, 2 h, 4 h, and 6 h (Scale-bar is 4 µm).

Based on the analysis of Fig. 1b-1f, it also shows that AgNO$_3$ nanoparticles have spherical morphology. The growth distribution of AgNO$_3$ nanoparticles formed is more bad-aligned with increasing growth time, evidenced by the presence of several gaps that are not overgrown by nanoparticles. All particles have a porous structure, with sizes ranging from 0.82 μm to 2.24 μm, which is useful in absorbing dye molecules to optimize the excitation of electrons if used on DSSC (Irmansyah et al., 2008; Nadaek et al., 2012). The absorption value is increase with the concentration of silver nanoparticles in the film increased (Masakke et al., 2015).

This non-uniform particle shape can be caused by high temperatures. This is in line with previous research (Fatimah et al., 2014), which says that "this inhomogeneity is due to the presence of sintering, which is the crystal clustering due to high heating". This was shown in the previous research which said that the increase in growth time would affect particle size, where increasing the growth time the make the particle size also increased (Distyawan et al., 2013).

Table 1. Diameter and surface area of TiO2 particles

Name	Diameter Range (μm)	Average Surface Area (μm^2)	Number of Particles	Density (number / area (μm^2))
Sample 1	1.70 ± 0.53	8.58 ± 2.68	81	9.44
Sample 2	1.53 ± 0.54	8.44 ± 2.97	74	8.77
Sample 3	2.29 ± 0.67	9.95 ± 2.89	72	7.24
Sample 4	1.62 ± 0.48	9.35 ± 2.77	68	7.27
Sample 5	1.52 ± 0.50	8.65 ± 2.87	61	7.05

The surface area of the TiO$_2$ particles seen in Table 1. It shows that the surface area of the particles at the time of growth was 0.5 h and 1 h smaller than the other samples. Whereas in 2 hours, it has the biggest surface area. The difference in growth time given affects the size of TiO$_2$ particles that are formed. At 0.5 h the particle size was relatively stable, this can be seen in sample 1 having an average surface area of 8.58 ± 2.68 μm^2. While at one hour the size of the particle area was reduced to 8.44 μm2 ± 2.97 μm2. The increase in growth time will affect the number of silver nanoparticles that are grown. We have used time variations to the growth of silver nanoparticles, which were 0.5 h, 1 h, 2 h, 4 h, and 6 h. The time variation is used to determine the number of nanoparticles that are formed in each sample. It is also used to determine the density of the number of nanoparticles formed in TiO$_2$. This is in line with previous studies that used growth time at 0.5 h. Growth reaction continued with the peak reaction of silver nanoparticle formation continued until the 60 and 90 minutes (Masakke & Rasyid, 2015). Concerning the amount of TiO$_2$ nanoparticles formed, this will affect the growth density of TiO$_2$ nanoparticles. For the level of density of growth of particles. In sample 1 the density level reached 9.44 / μm2 as well as the sample with the highest density value.

Fig. 2 shows the graph of the wavelength (λ) and the % R (reflectance) values obtained from the Uv-Vis spectrophotometer. The output data from the Uv-Vis spectrophotometer will produce %R values that vary between each sample. After the % R-value is obtained, this is used to determine the parameter values of R, (1-R)^2, 2R, α, hv, and αhv. These parameters are used to determine the value of the bandgap energy. After the αhv^2 parameter values are obtained, the two parameters are then plotted into a graph of αhv^2 values. Horizontal linear lines are drawn and vertical linear lines from the graph are drawn. At a certain point in the linear line that has been drawn there is an intersection

point. This intersection point is called α. A values are obtained using the Kubelka-Munk equation (Karim et al., 2016). The value of the ordinate point α from sample 1 to sample 5 can be seen in Table 2.
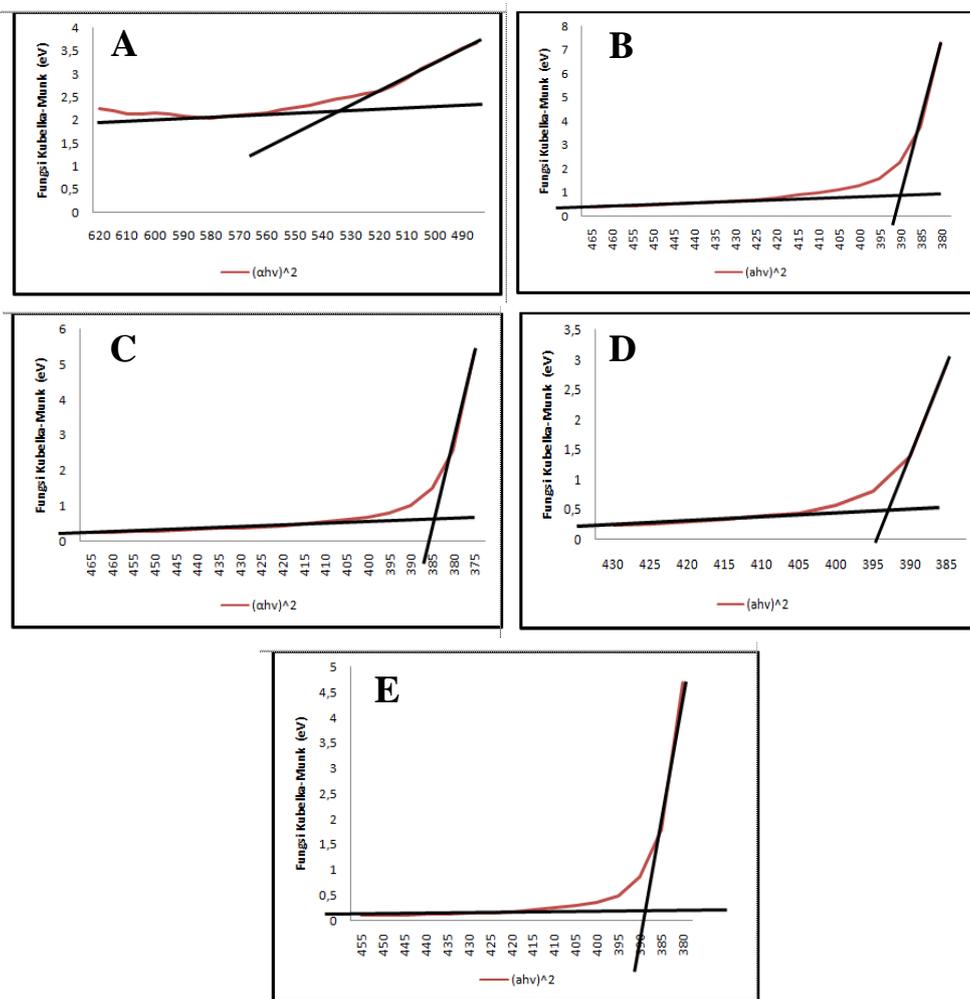
Figure 2. The α values for each sample (a) Sample 1, (b) Sample 2, (c) Sample 3, (d) Sample 4 and (e) Sample 5.

Table 2. The TiO₂ bandgap energy as an effect of AgNO₃ doped at the various growth time applications.

No	Name	Energy Band Gap Value
1	Sample 1	2.27 eV
2	Sample 2	1.08 eV
3	Sample 3	0.84 eV
4	Sample 4	0.47 eV
5	Sample 5	0.22 eV

The addition of AgNO₃ affects the gap value of the TiO₂ semiconductor energy band. This is similar to what was said by Cheng et al. (2016), "Doping significantly influences the absorption of light and bandgap energy". In sample 1 by growing TiO₂ by

doping $AgNO_3$ it has an energy band gap value of 2.27 eV, making electrons easier to move because the gap that is jumped is not too wide.

The results of the efficiency testing of the TiO_2 application in DSSC using the Gamry Instrument with TiO_2+AgNO_3/Dye/Plastisol structure are shown in Fig. 2. The details of the photovoltaic parameters of the DSSC performance with TiO_2 as photoanode are shown in Table 3. In sample 1 with a bandgap energy of 2.27 eV, resulting in the electrons can absorb photons better than other samples, resulting in the best efficiency. These results are similar to those shown in Table 3 data.

Table 3. The photovoltaic data of DSSC devices with TiO_2+AgNO_3/Dye/Plastisol structure.

Sample Name	Jsc (mA / cm²)	Eff (%)	FF	V_{oc} (mV)
Sample 1	0.943	0.285	0.435	0.694
Sample 2	0.825	0.227	0.446	0.616
Sample 3	0.657	0.201	0.431	0.706
Sample 4	0.531	0.148	0.463	0.599
Sample 5	0.553	0.098	0.363	0.488
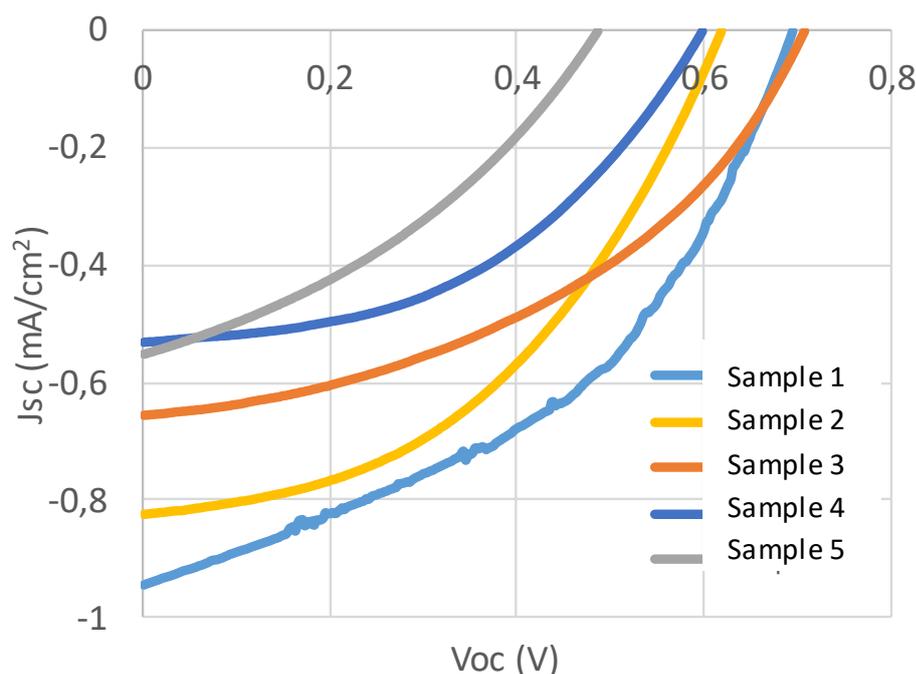
Figure 3. The J-V graph of DSSC devices with the structure of TiO_2+AgNO_3/Dye/Plastisol.

There was a very significant change in the value of the current density (Jsc) of each sample. The highest Jsc value was found in sample 1 which is equal to 0.943 mA /cm². The efficiency in sample 1 is the highest compared to others. The DSSC performance decreases with increasing in $AgNO_3$ growth time. The best DSSC performance with the use of TiO_2 as a photoanode doped by silver nanoparticles is 2.85×10^{-1}%. This efficiency result is 140 times greater than Anita et al. (2013), by using chlorophyll long bean leaves as a dye with a conversion efficiency of 2×10^{-3}%. But this performance is still far smaller compared to Grätzel (2003), by using a synthetic dye which reaches 11%.

CONSLUSSION

There is an influence of the TiO_2 microstructure formed with variations of growth time for 0.5 h, 1 h, 2 h, 4 h, and 6 h. The nanoparticles formed have a spherical microstructure with almost the same shape in each sample. The longer the growth time of TiO_2 nanoparticles by doping $AgNO_3$, the greater the size of the nanoparticles formed. This is in line with the number of nanopores formed on TiO_2 nanoparticles. With the least nanopores formed, the absorption of dye will be less, resulting in the efficiency of DSSC devices also decreases. This statemen also in line with the bandgap energy were decrease with the increase of $AgNO_3$ growth time. The most optimum DSSC device performance is 0.285% with an open voltage (Voc) of 0.694 V, current density (Jsc) of 0.943 mA / cm2, and a fill factor (FF) of 43.50% produced by the first sample as photoanode on the DSSC device.

ACKNOWLEDGMENTS

REFERENCES

Anita, A., Boisandi, B., Nurussaniah, N., Cari, C., & Suharyana, R. (2013). *Karakteristik Klorofil Pada Daun Kacang Panjang (Vigna Sinensis) sebagai Dye-Sensitized Solar Cells.* Paper presented at the lpf2013.

Asahi, R., Morikawa, T., Ohwaki, T., Aoki, K., & Taga, Y. (2001). Visible-light photocatalysis in nitrogen-doped titanium oxides. *Science, 293*(5528), 269-271.

Cheng, C.-K., Lin, C.-H., Wu, H.-C., Ma, C.-C. M., Yeh, T.-K., Chou, H.-Y., . . . Hsieh, C.-K. (2016). The two-dimensional nanocomposite of molybdenum disulfide and nitrogen-doped graphene oxide for efficient counter electrode of dye-sensitized solar cells. *Nanoscale research letters, 11*(1), 117.

Distyawan, A., & Susanti, D. (2013). Pengaruh Temperatur, Massa Zink, Substrat Dan Waktu Tahan Terhadap Struktur Dan Morfologi Zno Hasil Sintesis Dengan Metode Chemical Vapour Transport (CVT). *Jurnal Teknik ITS, 2*(2), F336-F341.

Ekasari, V., & Yudoyono, G. (2013). Fabrikasi DSSC dengan dye ekstrak jahe merah (Zingiber officinale linn var. rubrum) variasi larutan TiO2 nanopartikel berfase anatase dengan teknik pelapisan spin coating. *Jurnal Sains dan Seni ITS, 2*(1), B15-B20.

Fatimah, S., & Haris, A. (2014). Pengaruh Dopan Zink Oksida pada TiO2 terhadap Penurunan Kadar Limbah Fenol dan Cr (VI) secara Simultan dengan Metode Fotokatalisis. *Jurnal Kimia Sains dan Aplikasi, 17*(3), 86-89.

Grätzel, M. (2003). Dye-sensitized solar cells. *Journal of photochemistry and photobiology C: Photochemistry Reviews, 4*(2), 145-153.

Irmansyah, I., Maddu, A., & Zuhri, M. (2008). Fabrication and Characterization Dye-Sensitized Solar Cell based on TiO2/SnO2 Composit Electrode and Polymer Electrolite. *Jurnal ILMU DASAR, 9*(2), 96-103.

Kao, C.-C., Kuo, H.-C., Yeh, K., Chu, J., Peng, W., Huang, H., . . . Wang, S. (2007). Light–output enhancement of nano-roughened GaN laser lift-off light-emitting diodes formed by ICP dry etching. *IEEE Photonics Technology Letters, 19*(11), 849-851.

Karim, S., Pardoyo, P., & Subagio, A. (2016). Sintesis dan Karakterisasi TiO2 Terdoping Nitrogen (N-Doped TiO2) dengan Metode Sol–Gel. *Jurnal Kimia Sains Dan Aplikasi, 19*(2), 63-67.

Masakke, Y., & Rasyid, M. (2015). Biosintesis Partikel-nano Perak Menggunakan Ekstrak Metanol Daun Manggis (Garcinia mangostana L.). *Sainsmat: Jurnal Ilmiah Ilmu Pengetahuan Alam, 4*(1).

Mo, S.-D., & Ching, W. (1995). Electronic and optical properties of three phases of titanium dioxide: Rutile, anatase, and brookite. *Physical Review B, 51*(19), 13023.

Nadaek, S. M., & Susanti, D. (2012). Variasi temperatur dan waktu tahan kalsinasi terhadap unjuk kerja semikonduktor TiO2 sebagai dye sensitized solar cell (DSSC) dengan dye dari ekstrak buah naga merah. *Jurnal Teknik ITS, 1*(1), F81-F86.

Septina, W. (2007). Sintesa Nanokristal Mesopori TiO2 dengan Metoda Sol-Gel: Bandung: Institut Teknologi Bandung.

Šileikaitė, A., Prosyčevas, I., Puišo, J., Juraitis, A., & Guobienė, A. (2006). Analysis of silver nanoparticles produced by chemical reduction of silver salt solution. *Mater. Sci, 12*(4), 1392-1320.

Umar, A. A., Saad, S. K. M., Umar, M. I. A., Abd Rahman, M. Y., & Oyama, M. (2018). Advances in porous and high-energy (001)-faceted anatase TiO2 nanostructures. *Optical Materials, 75*, 390-430.

Umar, M. I. A. (2019). Graphene-Au Film Synthesized from GrO in Au-Aquaeus Solution as Counter Electrode For DSSC Application. *Lensa: Jurnal Kependidikan Fisika, 7*(2), 24-30.

Umar, M. I. A., Yap, C. C., Awang, R., & Salleh, M. M. (2017). Effect of thermal reduction temperature on the optical and electrical properties of multilayer graphene. *Journal of Materials Science: Materials in Electronics, 28*(1), 1038-1041.

Zamrani, R., & Gontjang, P. (2013). Pembuatan Dan Karakterisasi Prototipe Dye Sensitized Solar Cell (DSSC) Menggunakan Ekstraksi Kulit Buah Manggis Sebagai Dye Sensitizer Dengan Metode Doctor Blade. *Jurnal Sains Dan Seni Pomits, 1*(2).